J. Fluid Mech. (1975), *vol.* 71, *part* 1, *pp.* 145–160
Printed in Great Britain

The effects of wake splitter plates on bluff-body flow in the range $10^4 < R < 5 \times 10^4$. Part 2

By C. J. APELT AND G. S. WEST
Department of Civil Engineering, University of Queensland, Brisbane

(Received 11 November 1974)

The work reported in part 1 has been extended to cover flows past circular cylinders with wake splitter plates having $2 \leqslant L/D \leqslant 7$ and to include flows past normal flat plates with splitter plates having $L/D \leqslant 3{\cdot}7$. Pressure distributions and wake Strouhal numbers were measured and visualization studies carried out. The results obtained indicate that no further changes would be produced by lengthening the splitter plates beyond the limits tested.

The combined results of parts 1 and 2 provide coherent descriptions of the effects of wake splitter plates for all values of L/D of significance for the two profiles, which are representative of two distinct classes of bluff bodies, viz., those with cross-sections of curvilinear shape for which the flow separation points are not determined uniquely by the geometry and those for which the separation points are fixed.

1. Introduction

The effects of splitter plates placed along the centre-line of the wake of a circular cylinder in cross-flow at subcritical Reynolds numbers ($10^4 < R < 5 \times 10^4$) have been reported in detail by Apelt, West & Szewczyk (1973, hereafter referred to as part 1) for splitter plates having the proportions $L/D \leqslant 2$. It was found that splitter plates in this range caused a reduction in the drag on the cylinder, an increase in the base pressure, narrowing of the wake and a change in the Strouhal number for vortex shedding, compared with the values for a plain cylinder. The greatest effects on the drag coefficient C_D and base pressure coefficient C_{pb} were observed for $L/D = 1$, but even very short plates ($L/D = \frac{1}{16}$) caused marked changes in C_D and C_{pb}. It was concluded that the action of splitter plates for which $L/D \leqslant 1$ was to stabilize the separation points on the cylinder progressively and to reduce the wake width with increasing L/D.

The work reported in part 1 has been extended in two ways.

(i) The effects of long splitter plates in the wake of a circular cylinder have been investigated for $L/D \leqslant 7$. Pressure distributions, Strouhal numbers and velocity profiles were measured and visualization studies carried out. The experimental results indicate clearly that splitter plates with $L/D > 7$ will produce no further significant change.

(ii) In addition, pressure distributions and Strouhal numbers were measured for a two-dimensional flat plate set normal to the flow with a similar range of

splitter plates attached to it. These further experiments were carried out to compare the behaviour for two distinctly different types of bluff profile, viz., the flat plate, with fixed separation points, and the rounded circular profile.

2. Experimental work

The experimental techniques described in part 1 were used again with few changes. Pressure plotting and visualization studies were carried out in the water tunnel, measurements of the Strouhal frequency and velocity profiles with a hot-wire anemometer in the wind tunnel. Over the Reynolds number range 10^4–5×10^4, pressure distributions and Strouhal numbers were found to be independent of the Reynolds number and, consequently, visualization studies were made and velocity profiles measured at one characteristic Reynolds number only. The instrumentation described in part 1 was improved by the use of a more precise multi-tube manometer bank and a storage-type oscilloscope, which greatly simplified measurement of frequency.

The circular cylinder, 16 mm in diameter, was the same as that used in part 1 except that the pressure tappings were opened out to a diameter of 1·5 mm to give a more rapid response, tests reported in part 1 having shown that results for the pressure distribution were the same for tapping holes of diameters of 0·9 and 2 mm. Long splitter plates 1·5 mm thick were made to fit the existing groove in the base of the cylinder and were supported at the trailing edge to prevent oscillations owing to the fluctuating lift forces, the tips being held in adjustable clamps at the tunnel walls, the centre by a thin wire stay from tunnel floor to roof. The area blockage ratio was 6 %.

The flat plate was brass with a smoothly polished surface. It was 30 mm wide and 6 mm thick, with the edges machined to a sharp 45° bevel. Thirteen pressure tappings were spaced across the plane upstream face, with the outermost 1·5 mm from the edge of the plate, and six tappings were distributed over the rear surface. All pressure tappings were 1·5 mm in diameter and the pressure take-off tubes were carried inside the model. The ends of the model were sealed into the tunnel walls and the splitter plates were firmly located in a groove in the centre of the rear face of the model. The area blockage was $11\frac{1}{2}$ %, which is rather large, but this was the minimum model size that would accommodate all the pressure tappings deemed necessary. The wake widened quickly downstream from the flat plate, so that wake blockage effects are likely to be significant.

The velocity field near the circular cylinder was investigated in two ways. First, a DISA hot-wire anemometer probe was traversed through the wake and the mean and r.m.s. velocity components $\bar{u}$ and u' were measured. Near the splitter plate, where the flow direction reversed, the results were disregarded since the calibration is not valid for both flow directions. Second, a simple, very light, 'wool tuft' probe was traversed in a similar fashion. This gave a very clear indication of the outer edge of the shear layer, when it first became agitated, and of the region of reversed flow. The wool-tuft measurements were intended primarily to check the interpretation of the hot-wire results in the region of flow reversal.

Wake frequencies were measured using the hot-wire probe, usually positioned about $3D$† downstream and $2D$ away from the centre-line, and displayed on the oscilloscope. The signal was stored and subsequently measured, numerous repetitions being made for each model and Reynolds number.

Correct alignment of the models was an important factor in obtaining satisfactory results. At first it was thought that this could be achieved for the cylinder in the same way as for a plain cylinder, by rotating it until the pressures at $\pm 30°$ became equal, a method which had proved to be very satisfactory for models with short splitter plates. With long plates results obtained in this way were poor: base pressures and drag coefficients varied in a random fashion. Initially these variations were thought to be a Reynolds number effect, but it was then discovered that results could not be repeated to any degree of accuracy after re-rigging the model. After the alignment procedure had been refined, the random variations disappeared, results could be repeated at will and it was established that there was no variation with Reynolds number over the range

$$10^4 < R < 5 \times 10^4$$

for all model configurations tested. The following facts emerged.

(*a*) For $L/D < 3$, the simple alignment procedure was perfectly adequate, a misalignment of the cylinder of $\frac{1}{2}°$ being immediately apparent.

(*b*) For $5 > L/D > 3$, the pressure field could be balanced everywhere only by successive adjustment of the orientation of the cylinder and of the trailing edge of the splitter plate until the pressure readings at $\pm 30°$ and at $\pm 170°$ were equal.

(*c*) For $L/D \geqslant 5$, alignment was achieved by adjustment of the trailing edge of the splitter plate only. Rotation of the cylinder by as much as $\pm 10°$ had no effect, the pressure field rotating with the cylinder. This is illustrated in figure 1.

(*d*) The effect of raising the tip of the splitter plate (figure 2) varied with the length of the splitter plate: for $L/D \leqslant 6$ the pressures at P and N decreased, but for $L/D > 6$ they increased when the tip of the splitter plate was moved in the direction shown in figure 2.

The visualization experiments were recorded by means of the photographic technique described in part 1. For the circular cylinder three exposures were made of each model configuration: a direct side view to show any coupling between top and bottom, an oblique view of the flow over the plate and a side view of the wake some 15 diameters downstream of the model. For the flat plate, the near wake only was photographed; because of the rapid increase in wake width downstream nothing else of interest could be detected through the available observation windows.

3. Results

Pressure distributions in terms of C_p were derived from the piezometer readings, C_p being defined as $(p-p_0)/(p_s-p_0)$, where p is the pressure on the surface of the model, p_s the stagnation-point pressure and p_0 the static pressure

† The symbol D is used to denote both the diameter of the circular cylinder and the width of the flat plate.

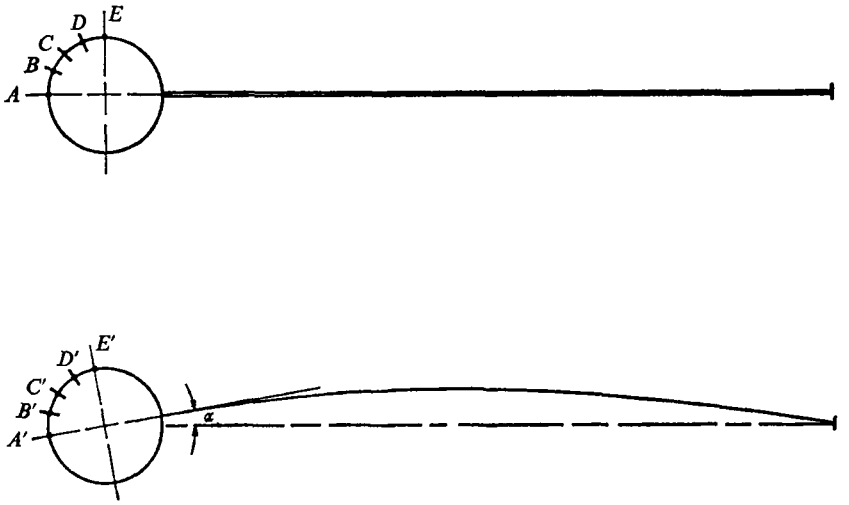

FIGURE 1. Permissible misalignment with long splitter plates. With $\alpha < 10°$, identical pressures are recorded at A and A', B and B', etc.

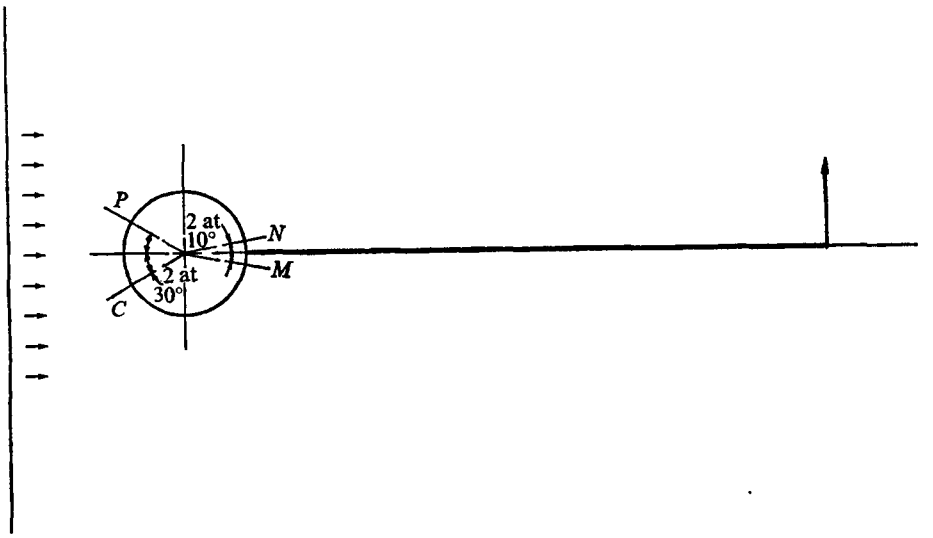

FIGURE 2. Effect of misplacing the trailing edge of the splitter plate.

in the empty working section at the position of the model. p_0 was calculated from static pressures measured at each end of the working section, the variation being treated as linear. The static taps were one tunnel diameter upstream from the model and four tunnel diameters downstream. Direct measurements of p_0 with the working section empty confirmed that the value obtained by linear interpolation was accurate.

Pressure distributions were measured over each model at five speeds giving a range of Reynolds numbers $10^4 < R < 5 \times 10^4$. The values of C_p for a given configuration were identical for all speeds. The pressure drag coefficient for each

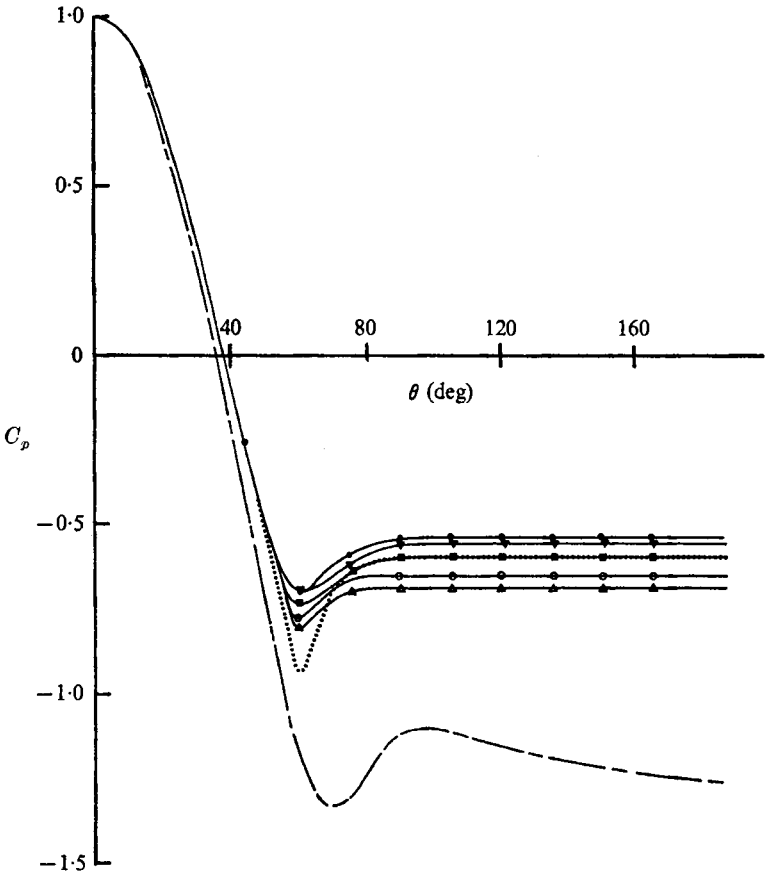

FIGURE 3. Circular cylinder: C_p *vs.* θ. ———, plain cylinder. With splitter plates: △, $L/D = 2\frac{1}{2}$; ○, $L/D = 3$; ■, $L/D = 3\frac{1}{2}$, 4; ·····, $L/D = 4\frac{1}{2}$; ▼, $L/D = 5$; ●, $L/D = 5\frac{1}{2}$, 6, $6\frac{1}{2}$, 7.

configuration is, therefore, independent of the Reynolds number in this range. The results obtained for the pressure distribution, base pressure and drag coefficient are shown in figures 3–6, which also include the results from part 1 for shorter splitter plates ($L/D < 2$) for completeness. From the pressure distributions it can be seen that on both the circular cylinder (figure 3) and the flat plate (figure 5) the base pressure is constant over the rear of the model. The pressure distribution on the front part of the circular cylinder over the region up to $\pm 38°$ is independent of the length of the splitter plate for $L/D \geqslant 2$. The pressure distribution on the upstream face of the flat plate where measurements were taken† is independent of the splitter-plate length for all results presented in figure 5, i.e. for $L/D \leqslant 3{\cdot}74$. The variations in the drag coefficient C_D and base pressure coefficient C_{pb} with splitter-plate length are shown for the circular cylinder in figure 4 and for the flat plate in figure 6. It should be noted that the drag coefficient presented in all cases is the pressure drag coefficient obtained by

† The locations at which measurements were made on the upstream face are shown by the data points in figure 5.

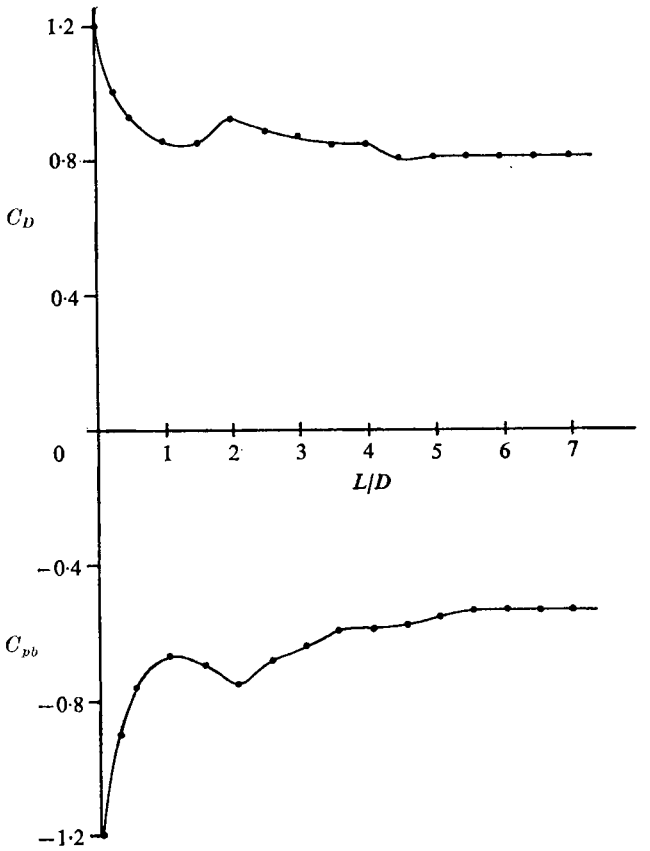

FIGURE 4. Circular cylinder with splitter plates: C_D and C_{pb} *vs.* L/D.

integration from the pressure distribution; the contributions to the drag from the shear stresses on the bluff body and on the splitter plate are not included.

Wake frequences are shown in figure 7 in the form Strouhal number

$$S = (fD/U) \textit{ vs. } L/D,$$

where f is the frequency of vortex shedding and D represents the cylinder diameter or plate width. Again, the results for shorter splitter plates from part 1 are included. For both the cylinder and the flat plate the longer splitter plates inhibited the formation of a regular vortex pattern over the splitter plate, but the oscilloscope trace still exhibited a dominant frequency. This dominant shedding frequency was measured and found to vary with time, for a given model. The ranges of splitter-plate lengths for which these phenomena were observed correspond to the regions shown dotted in figure 7. Some typical traces of the hot-wire signal for the circular cylinder in these regions are shown in figure 8. The minimum ratio L/D that prevents perfectly regular vortex shedding is 4 in the case of the circular cylinder and $2\frac{1}{2}$ for the flat plate.

Upstream effects. It was observed that, if the hot-wire probe was positioned upstream of the model, the oscilloscope trace was similar to that obtained downstream but with a much smaller amplitude. The greatest amplitude of the

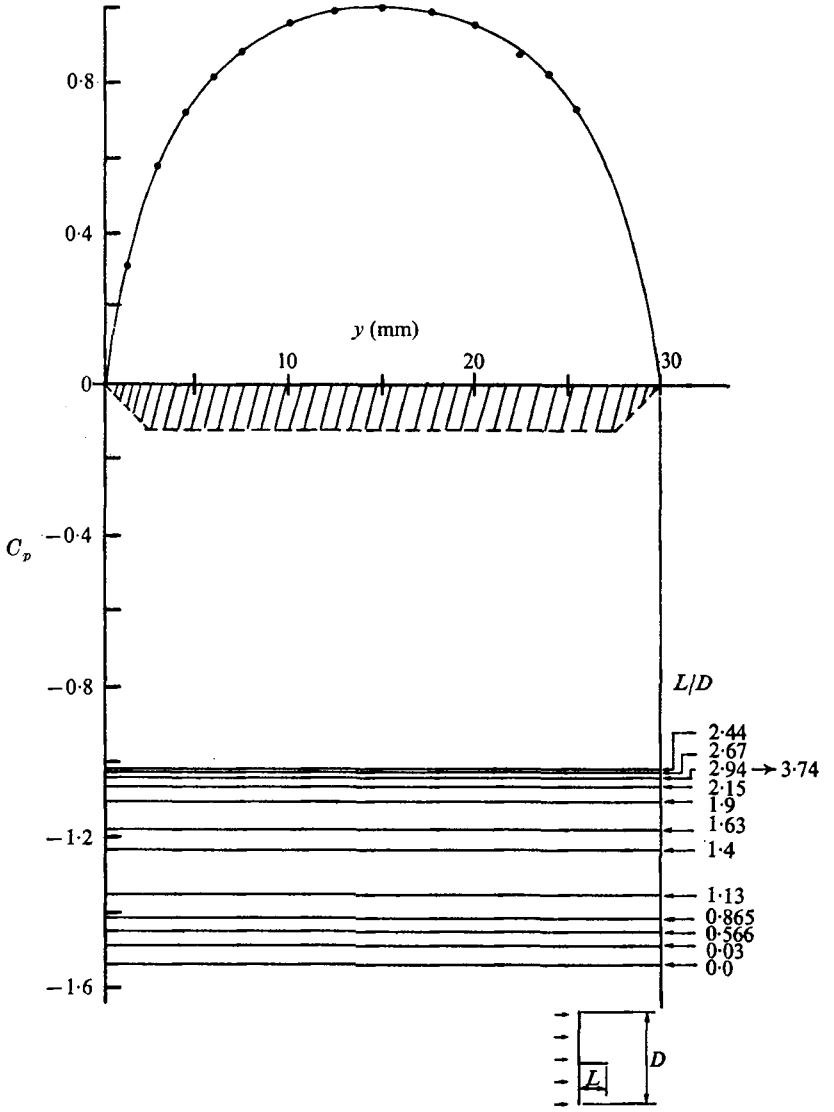

FIGURE 5. Normal flat plate with splitter plates: pressure distribution.

upstream signal was about 10 % of the downstream one and decreased across the flow to zero on the model centre-line in an approximately linear fashion. This effect extended upstream from the model for a distance of approximately $8D$ for both the cylinder and the flat plate.

Velocity profiles are plotted for the circular cylinder in figure 9 in the form $\overline{u}/U$, where $\overline{u}$ is the local mean velocity and U the velocity of the approaching stream. Approximately 20 points have been plotted on each curve between the undisturbed flow and the wake centre-line and lines drawn through the points with no attempt at smoothing. The curves are cut off where the mean velocity $\overline{u}$ reverses.

Some aspects of the structure of the wake of the cylinder/splitter-plate

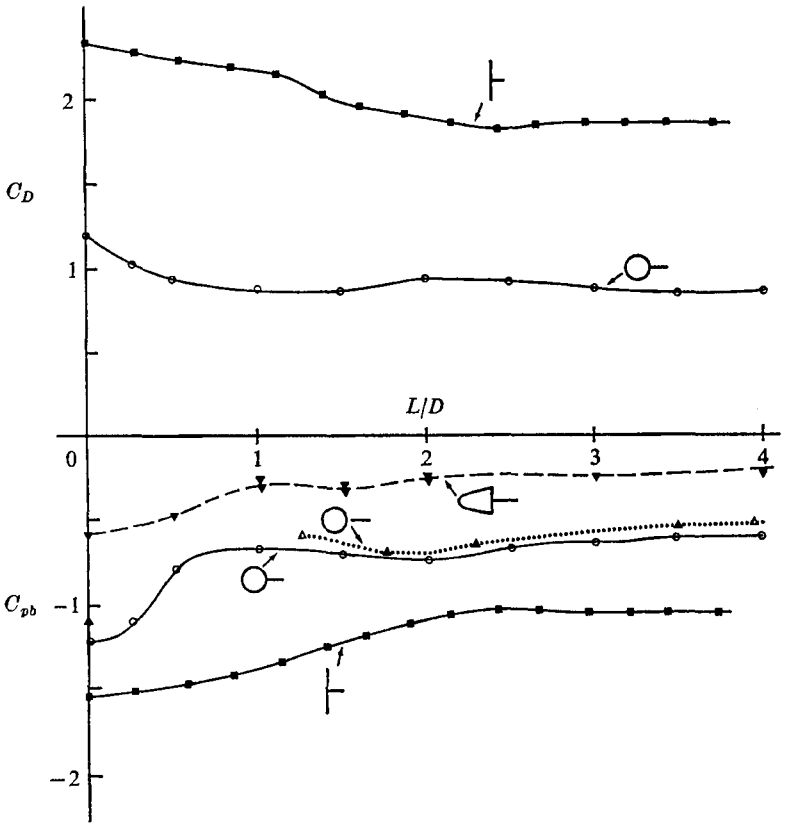

FIGURE 6. Comparison of results for circular cylinders and normal flat plates: C_D and C_{pb} *vs.* L/D. Results for Bearman's D-section and Roshko's cylinder with detached splitter plate are shown as dashed and dotted curves respectively.

combination are illustrated in figure 10. The innermost contour in each diagram represents the dividing line between forward and reversed flow as detected by the simple wool-tuft probe. This is a mean line which undergoes some slight excursions with time. The divided flow past the cylinder rejoins downstream from the trailing edge of the splitter plate for $L/D < 5$, but for splitter plates longer than this the flow reattaches to the splitter plate. The point of reattachment appears to be virtually independent of the length of the splitter plate in this latter case and is located a distance approximately $5D$ downstream from the centre of the cylinder. It seems that there is a connexion between the observed difficulty in alignment of the model and the position of the reattachment point relative to the splitter plate: alignment is controlled at the cylinder when the point of reattachment is downstream from the splitter plate but is controlled by the trailing edge of the plate when reattachment is on the splitter-plate surface.

The next two contours in each diagram in figure 10 are, respectively, lines joining the maximum values of u' and of $\bar{u}$, u' being the r.m.s. value of the turbulent velocity fluctuations. The manner in which these two contours diverge downstream was found to be related to the increase in the size and transverse

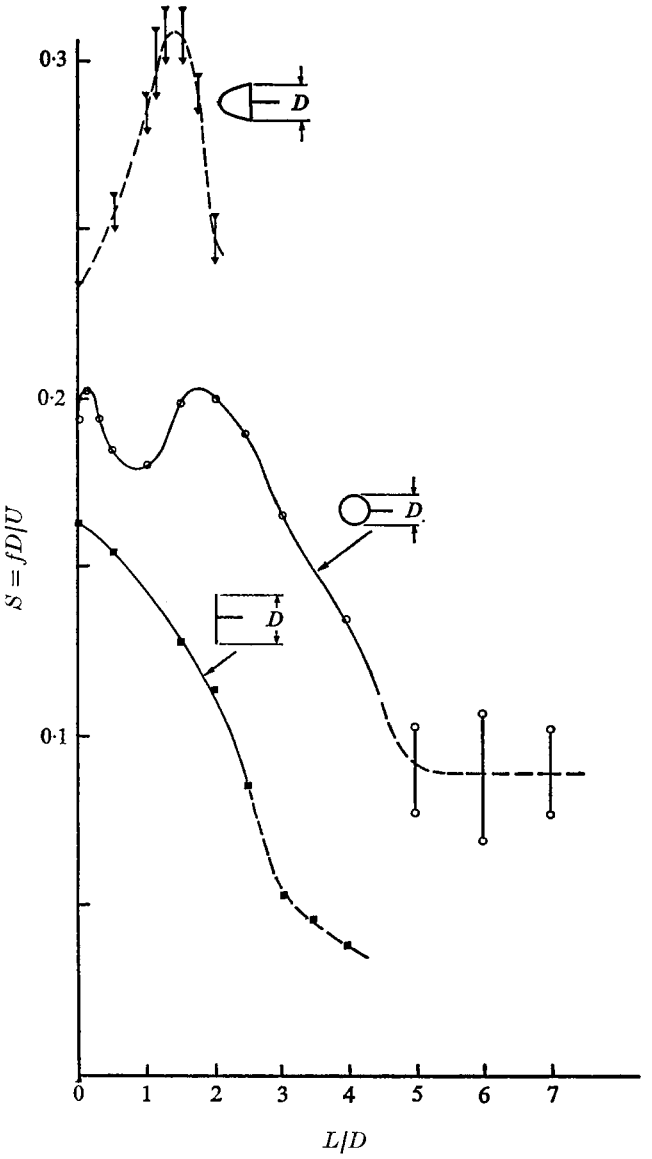

FIGURE 7. Variation of Strouhal number with L/D.

spacing of the vortices shed into the wake, as observed on the ciné films obtained during the visualization experiments.

A brief summary of the most obvious developments in the flow patterns traced by the dye in the visualization experiments is now given.

Circular cylinder. For $L/D = 2\frac{1}{2}$ and 3, the separated shear layers, which are laminar at separation, undergo transition further downstream and roll up into large vortices, perfectly coupled between the two sides of the plate, which depart alternately downstream, as for $L/D \leqslant 2$. The dye outline over the plate consequently oscillates up and down as the vortices break away. Over the plate the

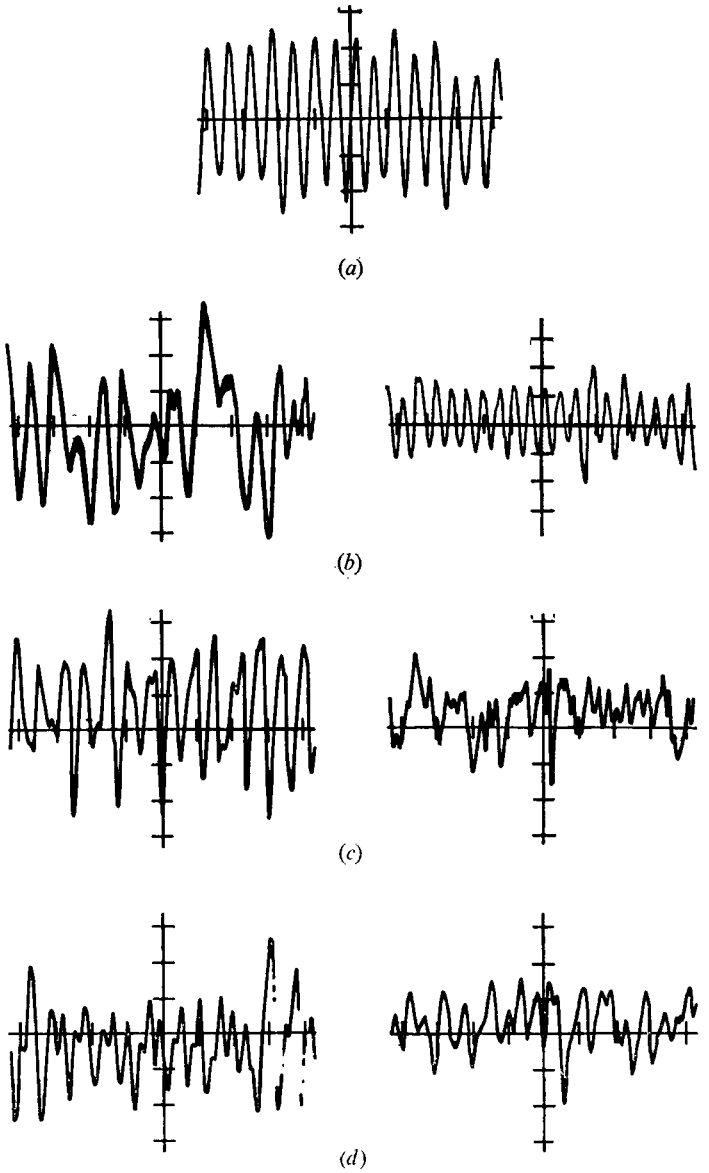

FIGURE 8. Some oscilloscope traces of anemometer signal in the near wake of the circular cylinder. Probe at $x = 3D$, $y = 2D$. (a) $L/D = 0$, (b) $L/D = 5$, (c) $L/D = 6$, (d) $L/D = 7$.

flow direction is reversed and near the cylinder it is almost stagnant. Immediately downstream a regular vortex street is clearly discernible but rapidly dissipates into a general wake pattern.

For $L/D = 3\frac{1}{2}$–$4\frac{1}{2}$, the size of the vortices produced over the plate is less than for shorter plates, so that the dye outline is much steadier. Coupling between the two sides of the plate is still evident but is now imperfect. A somewhat irregular vortex street forms immediately downstream of the model.

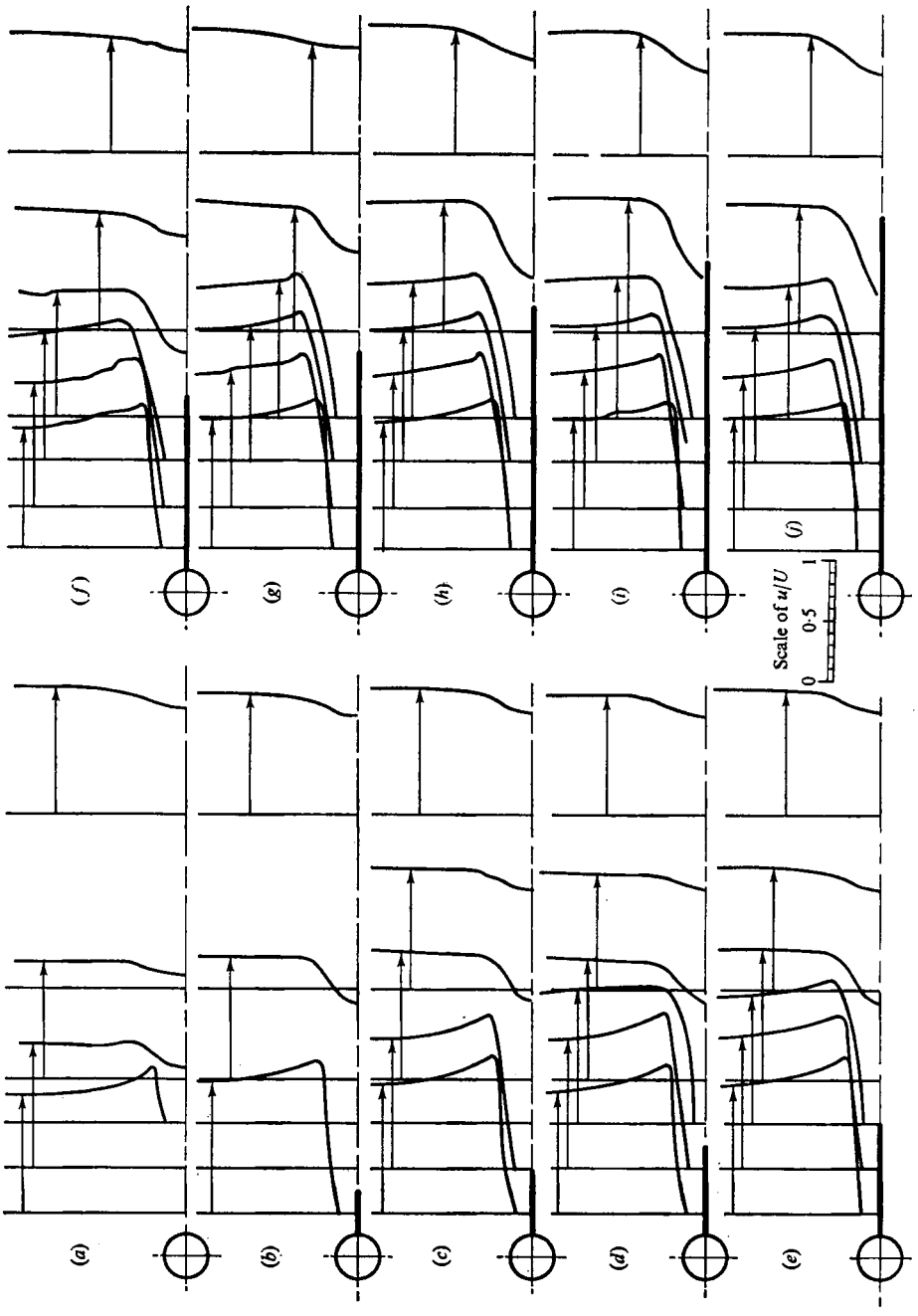

FIGURE 9. Circular cylinder: wake velocity profiles. Mean component $\overline{u}/U$. (*a*) $L/D = 0$, (*b*) $L/D = 1$, (*c*) $L/D = 1\frac{1}{2}$, (*d*) $L/D = 2$, (*e*) $L/D = 2\frac{1}{2}$, (*f*) $L/D = 3$, (*g*) $L/D = 4$, (*h*) $L/D = 5$, (*i*) $L/D = 6$, (*j*) $L/D = 7$.

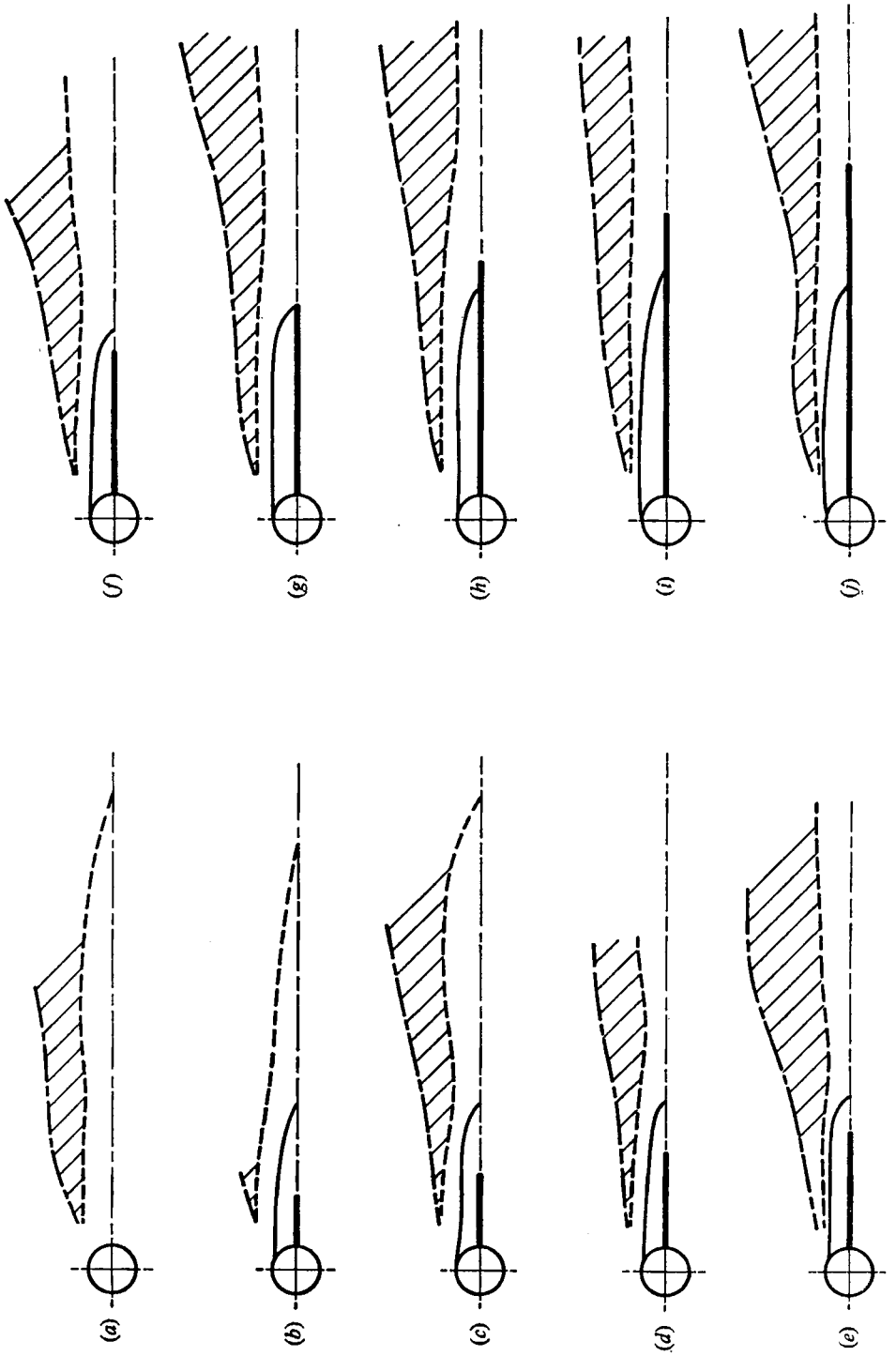

FIGURE 10. Wake contours. ——, $\bar{u}$ reverses; – – – –, u' is a maximum; — — —, $\bar{u}$ is a maximum. (*a*) $L/D = 0$, (*b*) $L/D = 1$, (*c*) $L/D = 1\frac{1}{2}$, (*d*) $L/D = 2$, (*e*) $L/D = 2\frac{1}{2}$, (*f*) $L/D = 3$, (*g*) $L/D = 4$, (*h*) $L/D = 5$, (*i*) $L/D = 6$, (*j*) $L/D = 7$.

For $L/D = 5$–7, the vortices forming over the plate are very small and random with no coupling between the two sides. The wake envelope is, consequently, steadier and narrower. The flow reattaches to the plate at approximately $5D$ downstream of the cylinder regardless of the splitter-plate length, with reversed flow upstream of the reattachment line. There is a well-formed vortex street some distance downstream of the model; figure 11 (plate 1) shows a single frame from the film indicating the vortex centres clearly, at $x/D = 17$.

Normal flat plate. The above sequence is generally repeated. With no wake splitter plate there is a coupled vortex pattern with an oscillating wake profile. Splitter plates progressively modify this with increasing L/D, the alternate vortex shedding persisting as far as $L/D = 2$, but becoming erratic thereafter. With long plates ($L/D > 3$) the wake pattern is indistinguishable from that occurring behind the circular cylinder with splitter plates for which $L/D \geqslant 5$.

4. A note on blockage

None of the data presented has been corrected for blockage effects. There is real doubt whether any of the procedures currently in use for correction of blockage effects applies to the case of a bluff body with a splitter plate attached, and consequently it was judged best not to attempt to correct for blockage effects. The following relevant data are recorded so that blockage corrections can be made by interested readers when a suitable procedure for correction has been demonstrated.

Pressure measurements. The circular cylinder was 16 mm in diameter and 331 mm long, with 6 % area blockage. The flat plate was 30×331 mm long, with $11\frac{1}{2}$ % area blockage.

Velocity profiles and Strouhal numbers. The circular cylinder was 25 mm in diameter and 305 mm long, with 7 % blockage. The flat plate was 30×305 mm long, with 12 % blockage.

5. Discussion

There are evidently similarities between the effects of splitter plates on flow past the cylinder and the flat plate, viz., an increase in splitter-plate length is associated with progressive reduction in the drag and vortex shedding frequency until eventually a constant drag coefficient is reached and regular vortex shedding is eliminated. On the other hand, there are very obvious differences in behaviour when the splitter plate is short, and the flat plate shows no signs of the various flow regimes of the circular cylinder with $L/D < 2$ which have been reported in part 1. Generally, it may be deduced that, provided that the splitter plate is 'long', all bluff profiles have very similar flow patterns. The complexity of the effects of splitter plates on the flow about a rounded profile, demonstrated best in figure 7 for $L/D < 2$ but evident also in the undulations in figure 6, is caused by changes in the location of the separation points on the profile as has been discussed in part 1.

With long plates the changes are not as 'progressive' as figures 4 and 6 at first sight would indicate. The pressure distributions show that for each model there is a certain ratio L/D that has unique properties: for the circular cylinder it is $4\frac{1}{2}$,

when a singularly low value of C_p (checked very carefully in the water tunnel) exists around 60°, and for the flat plate it is $2\frac{1}{2}$, when C_{pb} is a minimum. These unique conditions produce the overall minimum drag in each case and seem to be associated with the rejoining or reattachment of the divided flow round the body. When the reattachment point is on the splitter plate, the latter can be regarded as 'infinitely long' since a further increase in its length has no effect on the flow pattern. The 'infinitely long' condition occurs for $L/D > 5$ for the circular cylinder and for $L/D \geqslant 3$ for the flat plate. This inference, drawn from the results for the pressure distribution and for C_D, is confirmed in the case of the circular cylinder by the data in figure 10, which show that the divided flow past the cylinder reattaches to the splitter plate for $L/D \geqslant 5$. For splitter plates which are shorter than the minimum values specified for the 'infinitely long' condition, the flow pattern, pressure distributions and C_D all vary with the length of the splitter plate. Further, figure 7 shows that regular vortex shedding cannot be said to be eliminated unless the splitter plate is 'infinitely long'. However, when such long splitter plates were attached to the cylinder, a well-developed vortex street was formed well downstream ($\sim 17D$), as illustrated in figure 11, even though there was no regular vortex shedding from the cylinder itself. In these cases it appears that the cylinder/splitter-plate combination gives rise to its own distinct vortex street far downstream.

The results of studies by Roshko (1954) and by Bearman (1965) are compared with those from the present investigation in figures 6 and 7. Roshko's experiments were done on a circular cylinder with a splitter plate of constant length ($1{\cdot}14D$) placed at different distances downstream in the wake of the cylinder, and the dimension L in his experiments is taken as the distance from the downstream edge of the splitter plate to the downstream generator of the cylinder. When allowance is made for the different blockage ratios in Roshko's experiments and those reported here, there is very good agreement between the results for C_{pb} from the two different studies. Bearman's model had a long streamlined upstream section which terminated abruptly at a rearward-facing plane surface, to which splitter plates of different lengths were attached; the geometry had similarities to that of a flat plate normal to the flow in that the separation points were fixed in each case, but in Bearman's experiments, the thickness of the separating shear layers was very large, being approximately half the distance between them. Nevertheless, the variation of C_{pb} with splitter-plate length in Bearman's experiments gives a curve in figure 6 which is similar in shape to that obtained for the normal flat plate even though the magnitudes are very different. Bearman found that the Strouhal number varied with Reynolds number for his model, which was not the case in the experiments reported here; presumably the dependence on Reynolds number in his experiments is associated with variations in the thickness of the separating shear layers.

The velocity profiles for flow past the cylinder in figure 9 enable the relationship between the base pressure coefficient and stream velocity U' at the outer edge of the wake to be investigated. If $U' = kU$, the pressure coefficient C_p associated with U' is given by $1-k^2$, and this is usually assumed equal to C_{pb}. Table 1 compares the values of U'/U from figure 9 and values of k calculated from the

Model	U'/U					
L/D	$x/D = 1$	$x/D = 2$	$x/D = 3$	$x/D = 4$	$x/D = 6$	$(1-C_{pb})^{\frac{1}{2}}$
0	1·27	1·07	—	1·05	—	1·48
$\frac{1}{2}$	1·36	—	—	1·08	—	1·33
1	1·35	—	—	1·09	—	1·29
$1\frac{1}{2}$	1·37	1·36	1·24	1·10	1·09	1·30
2	1·31	1·38	1·21	1·06	1·05	1·33
$2\frac{1}{2}$	1·35	1·32	1·25	1·12	1·07	1·30
3	1·29	1·28	1·25	1·10	1·07	1·29
4	1·36	1·31	1·30	1·26	1·09	1·26
5	1·32	1·33	1·28	1·26	1·12	1·25
6	1·32	1·33	1·32	1·26	1·15	1·25
7	1·33	1·33	1·31	1·23	1·13	1·25

TABLE 1

expression $k = (1-C_{pb})^{\frac{1}{2}}$, in which C_{pb} is the value measured on the surface of the model. The value of U' used was the maximum ordinate of the velocity profile and U is the approach velocity upstream from the model.

The results in table 1 show quite close agreement between the value of U'/U at $x/D = 1$ and the value of $(1-C_{pb})^{\frac{1}{2}}$ for splitter plates having $L/D \geqslant \frac{1}{2}$, thus providing support for the assumption that $C_{pu'} = C_{pb}$, i.e. that the base pressure is equal to the free-stream pressure at the edges of the shear layers. Similar studies by Simmons (1974) with bluff bodies having sharp separation points showed similar good correlations when U' was measured very close to the separation point.

6. Conclusions

Short splitter plates in the wake of a circular cylinder very significantly modify the characteristics of the flow past the cylinder. Even though short splitter plates have less effect on the flow past a normal flat plate, the effect is significant even when the splitter plate is very short.

Splitter plates longer than $2D$ in the wake of a circular cylinder progressively modify the drag and vortex shedding until $L/D = 5$. For $L/D > 5$ there is no further change; C_D is constant at 0·8 and vortex shedding from the cylinder is eliminated. However, a vortex street forms well downstream from the cylinder/splitter-plate combination.

Splitter plates in the wake of the normal flat plate modify the drag and vortex shedding monotonically as L/D increases from 0 to 3. No further change occurs for $L/D > 3$; C_D is constant at 1·84 and vortex shedding has ceased.

With very long splitter plates behind a circular cylinder ($L/D > 5$) the flow reattaches to the plate surface at approximately $5D$ downstream from the cylinder, regardless of the splitter-plate length. Once the reattachment point is on the plate surface, there is no further significant change in the flow pattern.

The assumption, frequently made, that the base pressure on the model is equal to the free-stream pressure just outside the wake has been tested and found to be quite accurate when splitter plates are fitted.

REFERENCES

APELT, C. J., WEST, G. S. & SZEWCZYK, A. A. 1973 The effects of wake splitter plates on the flow past a circular cylinder in the range $10^4 < R < 5 \times 10^4$. *J. Fluid Mech.* **61**, 187.

BEARMAN, P. W. 1965 Investigation of the flow behind a two-dimensional model with a blunt trailing edge and fitted with splitter plates. *J. Fluid Mech.* **21**, 241.

ROSHKO, A. 1954 On the drag and shedding frequency of two-dimensional bluff bodies. *N.A.C.A. Tech. Note*, no. 3169.

SIMMONS, J. E. L. 1974 The relationship between the base pressure on a bluff body and the velocity at separation. *Aero. J.* **78**, 330.

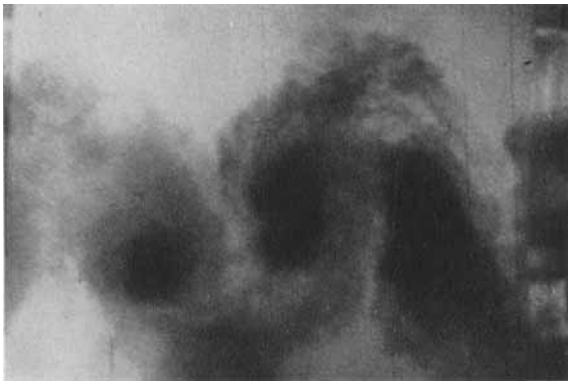

FIGURE 11. Vortex centres well downstream of a circular cylinder with a long splitter plate at $x/D = 17$.